UDC 621.373.8: 621.375.826

Quantum-dot Lasers Fabricated with Self-assembled Microcrystals

●Kohki Mukai ●Yoshiaki Nakata ●Mitsuru Sugawara
(Manuscript received June 8, 1998)

This paper describes improvements that have been achieved in the optical properties of self-assembled InGaAs quantum dots and the high performance of quantum-dot lasers that incorporate these improvements. We found that spectra broadening was reduced and emission efficiency was improved by alternately supplying small amounts of InAs and GaAs on GaAs substrates to grow quantum dots using both metalorganic vapor phase epitaxy and molecular beam epitaxy. The narrow spectra and high emission efficiency improve the practical performance of dot lasers. A threshold current of 5.4 mA, a current density of 160 A/cm^2, and an output power of 110 mW were achieved in continuous wave operation at 25°C.

1. Introduction

Three-dimensional quantum confinement of electrons, holes, and excitons in semiconductor microcrystals known as quantum dots is predicted to produce new physical phenomena[1),2)] and improve optoelectronic devices significantly.[3)-6)] The atom-like state density in quantum dots associated with three-dimensional confinement of electrons and holes[7)] would cause an increase of optical gain and limit thermal carrier distribution. Therefore, the use of quantum dots for semiconductor lasers as an active region is expected to provide a remarkable reduction of threshold current and temperature sensitivity. During primary research based on predictions in the early 1980s, quantum dots have been created by combining lithography and regrowth on a processed substrate.[8),9)] The artificial techniques, however, suffer from nonuniform dot size, poor interface quality, and low numerical density. High uniformity is required to achieve the atom-like state density of a dot ensemble. A high optical quality and high numerical density are required to obtain a large gain. Quantum dot lasers using artificial techniques, therefore, showed a high threshold current density (7,600 A/cm^2 at 77 K).[10)]

The strain-induced self-assembling technique was a breakthrough in the fabrication of quantum dots.[11)] Self-assembled quantum dots have uniform sizes, high numerical densities, and high emission efficiencies, none of which have been realized in the previous artificial techniques. The growth technique has been successfully applied to Si,[12)] SiGe,[13)] InAs,[14)] InGaAs,[15)-18)] InP,[19)] GaSb,[20)] InSb,[21)] CdSe,[22)] and GaN[23)] dots. Most well-known self-assembled dots are three-dimensional islands on a growth surface formed via the Stranski-Krastanov mode (SK dots), where the islands grow after the strain energy exceeds the critical limit of a two-dimensional structure (wetting layer). Using the InGaAs SK dots, the threshold current of dot lasers was reduced,[24)] and since then, it has been further improved year by year.[25)-28)] However, the predicted laser performances have not yet been achieved, because the size uniformity, numerical density, and emission efficiency of the self-assembled dots require further improvement.

This paper describes the high-performance

characteristics of quantum-dot lasers that were achieved by improving the properties of self-assembled dots. We used metalorganic vapor phase epitaxy (MOVPE) and molecular beam epitaxy (MBE) to grow the quantum dots, and found that the uniformity and emission efficiency were improved by growing dots through an alternate supply of InAs and GaAs on GaAs substrates. Using this growth technique in MBE, we achieved a record low threshold (5.4 mA) and a record high output power (110 mW) in edge-emitting quantum-dot lasers.

2. Growth of Self-assembled Quantum Dots

2.1 MOVPE growth

We grew self-assembled quantum dots with an alternate supply of precursors using a growth sequence of atomic layer epitaxy in a MOVPE chamber. The MOVPE system was designed for pulse jet epitaxy, in which source gases are supplied in a fast, pulsed stream.[18),29)] The source materials are trimethylindium-dimethylethylamine adduct (TMIDMEA),[30)] trimethylgallium (TMG), and arsine (AsH_3). The growth temperature was 460°C. We performed 14 to 18 cycles of In-Ga-As alternate supply separated by H_2 purging pulses on a GaAs buffer layer on a (001)GaAs substrate. To obtain a high emission intensity, the TMIDMEA amount for one cycle was optimized at a 0.5 monolayer (ML) and the TMG amount was optimized at a 0.06 ML. Because of the unique growth sequence, we named this type of dot the "ALS (alternate supply) dot." The structure of the ALS dot is quite different from that of the SK dot.

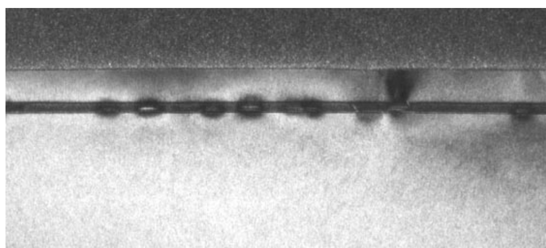

Figure 1
Cross-sectional TEM image of ALS dots.

Figure 1 shows a cross-sectional transmission electron microscopy (TEM) image of ALS dots which illustrates their unique structure. The figure shows InGaAs ALS dots surrounded by an InGaAs quantum well layer. The dots are about 10 nm high and 20 nm in diameter. The dot size is small enough for quantum-size effects (Bohr radius is about 20 nm in this material system).[31)] The indium composition of the dots and the surrounding quantum well were determined to be 0.5 and 0.1, respectively, by energy-dispersive X-ray microanalysis (EDX) with a spatial resolution of 1 nm. The areal coverage of the dots was 5 to 10%. The quantum well surrounding the dots has the same thickness as the dots and is more than 10 times thicker than the wetting layer of SK dots. The height of the ALS dots is half of their diameter, whereas the height of SK dots is less than a quarter of their diameter. The structural differences suggest that the growth mechanism of the ALS dots differ from the SK mode.

From the unique structure, we suppose that the ALS dots were formed as a compositional nonuniformity during a two-dimensional growth or segregation in bulk. The flat surface cannot be explained by assuming a three-dimensional growth. The growth temperature (460°C) and growth rate (1 monolayer per 10 s) were significantly smaller than those of ordinary MOVPE or MBE growth. The small growth rate and growth temperature enhance the surface-migration length of adatoms, leading to two-dimensional growth.[32)] Even if the In- or Ga-metal islands formed during the group-III atom's supply, the metal islands can deform to a monolayer structure during the group-V atom supply since the amount of group-III atoms in one supply cycle was for single or lower coverage.[33)] It is possible that atoms move to form microcrystals which reduce the enthalpy, since an $(InAs)_1/(GaAs)_1$ bulk monolayer superlattice is intrinsically unstable against phase segregation.[34)]

The optical characteristics of the ALS dots are more suitable for laser applications than those of ordinary SK dots. **Figure 2** compares the photoluminescence (PL) spectra of the ALS dots and SK dots grown by MBE. The PL measurements were performed with a 647.1 nm Kr^+ ion laser. Luminescence from the sample surface was monochromed by a 50 cm monochrometer and detected by a PbS detector using a conventional lock-in technique. From the figure, we can see that spectra broadening is smaller in the ALS dots than in the SK dots. The full width at half maximum (FWHM) of the ALS dots is 30 meV, while that of the SK dots is 80 to 100 meV. Since the state density of a single dot is delta-function-like, the spectra width reveals an inhomogeneous broadening of energy in the dot ensemble. Therefore, the result suggests that the ALS dots are more uniform than the SK dots. The emission wavelength of the ground level was longer for the ALS dots than for the SK dots. The ALS dots emit in the 1.3 μm region, which is practical for a fiber telecommunication system. We presume that the comparatively large height of the ALS dots makes the sublevel energy less sensitive to variation in dot height in the monolayer and also enables long-wavelength emission.

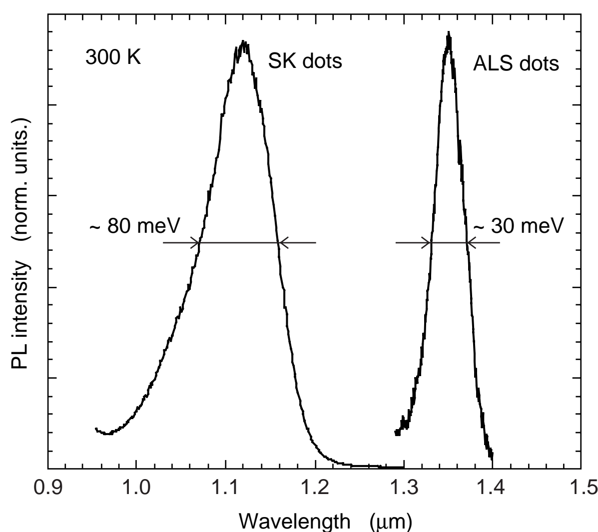

Figure 2
PL spectra of the ALS dots and SK dots.

As for optical quality, the ALS dots are also better than the SK dots. **Figure 3** shows the PL intensity (normalized to the low-temperature value) as a function of temperature. The PL intensity of the SK dots grown by MBE is shown as a reference. The figure shows that the PL intensity of the ALS dots decreased by approximately one order of magnitude as the temperature was increased to 300 K. By contrast, the intensity of the SK dots decreased by almost three orders of magnitude. There seems to be a critical temperature (about 150 K) where the slope inclination changed, suggesting that there were at least two sources of the PL intensity reduction in the SK dots.

The reasons for the superior PL intensity of the ALS dots over the SK dots may be due to their unique growth process. One reason is presumably the better interface quality around the ALS dots. The interface around the ALS dots is ambiguous since the dots were possibly self-formed during two-dimensional growth. The interface of the SK dots is abrupt since it is the border between the growth islands and the over-grown layer. Another reason is possibly in-situ annealing during the slow growth of the ALS dots. The

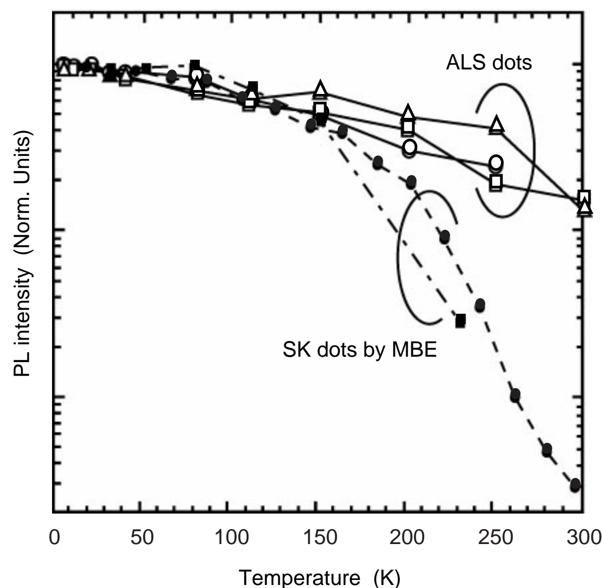

Figure 3
PL intensities of ALS dots and SK dots as function of temperature.

growth rate is significantly low. Since the growth temperature of 460°C is lower than the temperature at which arsenic desorption occurs at the growth surface,[35] some defects leave from the surface during the slow growth.

2.2 MBE growth

Dots with a high uniformity and high emission efficiency were also grown in a solid source MBE chamber by alternately supplying InAs and GaAs on a (001)GaAs substrate. The amount of source materials for one cycle differed from that for the ALS dots. The eight cycles of 0.7 ML InAs and 3 ML GaAs were performed after a single 1.8 ML InAs supply. The growth temperature was 510°C. **Figure 4** shows the resultant self-assembled quantum dots. In the figure, we can see two dots having a columnar shape. Because of the shape of this structure, we named these types of dots "columnar dots." Both the diameter and height of the columnar dots were about 15 nm. The areal coverage of the dots was 10 to 20%. Figure 4 also clearly shows the multiple wetting layers produced during each InAs supply. We therefore suppose that the growth mechanism of columnar dots differs from that of ALS dots. We consider that the columnar dots are a type of closely stacked dot, whereas the SK dots are stacked with a thin intermediate layer so as to couple electrically.[37)-39] From the growth condition (and because there is no clear multiple structure in the columnar dots), we assume that the islands produced during each InAs supply contact directly. Such a structure differs from ordinary closely-stacked dots.

Figure 5 compares the PL spectra of the columnar dots with those of the SK InAs dots and previously reported closely-stacked dots grown by stacking 1.8 ML InAs dots with 3 nm GaAs intermediate layers.[40] The emission wavelength of the ground level of the columnar dots was 1.17 µm and that of the second level was 1.1 µm. An emission peak related to the multiple wetting layers was observed at 1.01 µm. The emission wavelength of the wetting layers was longer than that of the SK dots. The wavelength of the single SK dots was 0.92 µm. We suppose that the emission wavelength is longer because the multiple wetting layers of the columnar dot were coupled electrically.

Two points deserve special attention in Figure 5. First, the emission intensity of the columnar dots is equal to that of the SK dots and quite improved compared to previously reported closely-stacked dots, which hardly emitted at room temperature. The PL intensity in the closely-

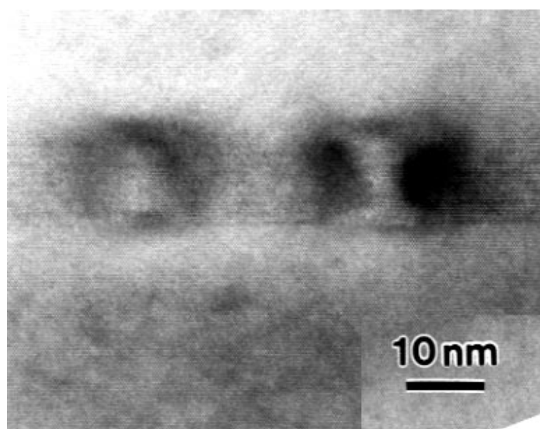

Figure 4
Cross-sectional TEM image of two columnar dots.

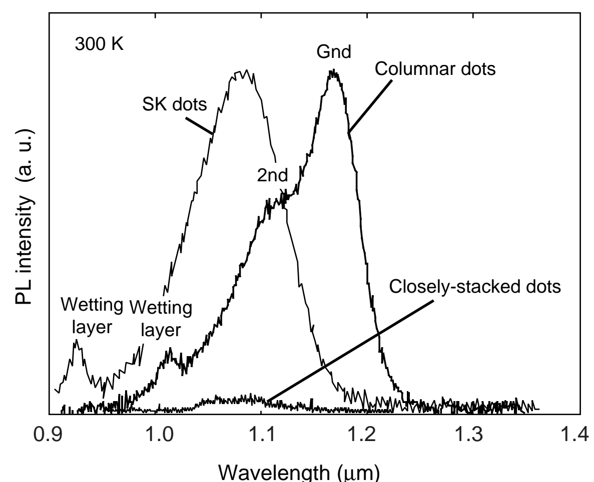

Figure 5
PL spectra of the columnar dots, SK InAs dots, and closely stacked dots.

stacked dots at room temperature was less than one thousandth of the intensity at 77 K. Second, the columnar dots have a narrower spectrum width than the SK dots. Due to the existence of excited levels, the improvement is not very obvious, but the peak width of the ground level is almost half that of the SK dots. The half width at half maximum (HWHM) in the spectrum is 20 to 25 meV for the ground level, which is significantly smaller than the 45 meV of the ordinary single SK dots (but larger than that of the ALS dots). The narrower spectrum suggests that the columnar dots have a better uniformity than the SK dots. We conjecture that the thick dot structure, as in the ALS dots, reduces the sensitivity to variation in dot height.

3. Performance of Quantum-dot Lasers

3.1 ALS-dot lasers

Figure 6 schematically shows the fabricated laser structure. An n-GaAs buffer layer (0.5 µm), an n-InGaP cladding layer (1.0 µm), a non-doped active layer (0.2 µm), a p-AlGaAs cladding layer (1.0 µm), and a p-GaAs cap layer (0.5 µm) were grown on a (001) n-GaAs substrate. Broad contact lasers with a cavity length of 900 µm were fabricated using this laser structure.

Measurements were done at 80 K by current injection under a pulsed condition (pulse width: 500 ns, repetition rate: 10 kHz). **Figure 7** shows the electroluminescence (EL) spectra for various injection currents. The light output versus injected current characteristics are shown in **Figure 8**.

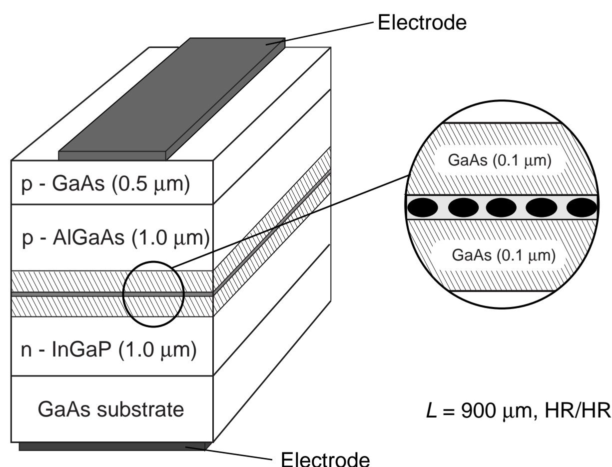

Figure 6
Schematic of the ALS-dot laser structure.

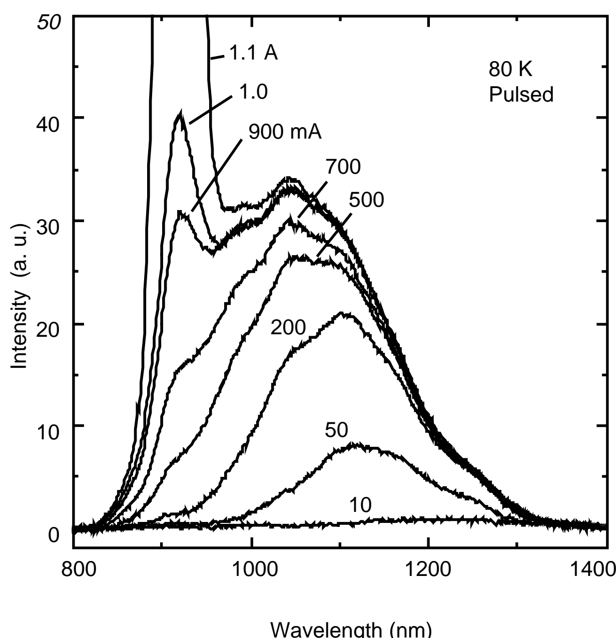

Figure 7
EL spectra of ALS-dot laser for various injection currents.

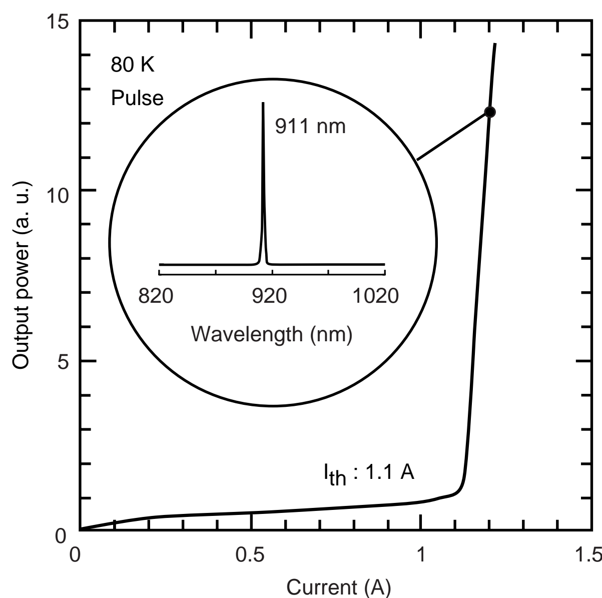

Figure 8
L-I characteristics of ALS-dot laser. Lasing spectrum is shown in inset.

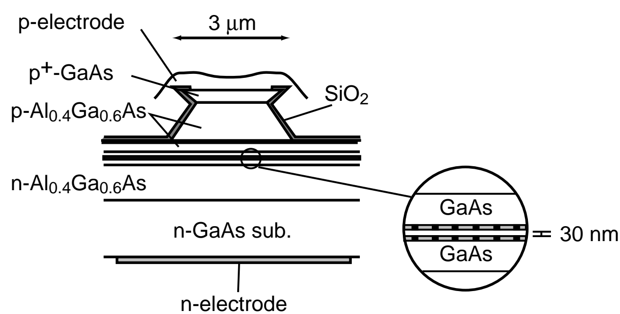

Figure 9
Schematic cross section of columnar-dot laser.

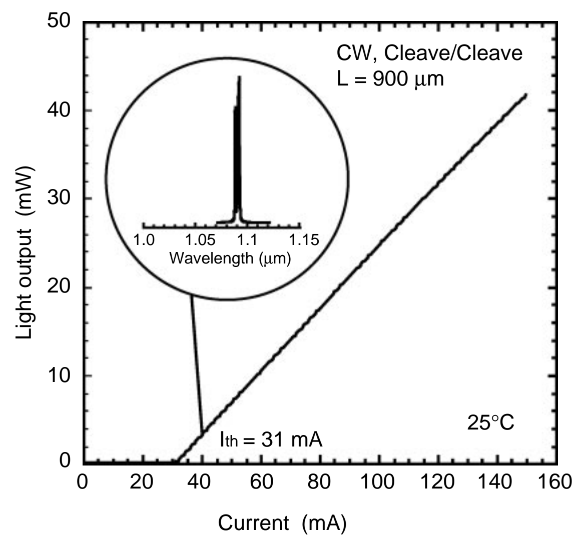

Figure 10
L-I characteristics of columnar-dot laser at 25˚C. Both facets were as-cleaved.

The peak broadening in the shorter wavelength region, which develops as the injection current is increased, is due to excitation of the sublevels. Band filling was observed with the current injection. The spectral intensity of each sublevel reflects the degeneracy of quantum levels, and the spacing of about 60 meV between the sublevels coincides with the theoretical estimation for the size of our quantum dots, in which a parabolic confinement potential is assumed.[18] We achieved laser oscillation at a threshold current of 1.1 A. Based on the near-field pattern, we estimated that the width of the current injection area was 150 µm, which gives a current density of 815 A/cm^2 at the observed 1.1 A threshold current. This current density is one-order of magnitude smaller than that of lasers built using artificially fabricated dots. As shown in the inset of Figure 8, the lasing wavelength was 911 nm. Considering that the compositional wavelength of the InGaAs barrier layer at 80 K is shorter than 850 nm, the laser oscillation is from a high-order sublevel of the ALS dots.

The observed EL spectra also indicate that the lowest level, at around 1.25 µm at 80 K, is filled with an extremely low current injection level (below 50 mA). This suggests that ultra-low threshold current density operation could be realized in quantum dot lasers. The laser oscillation occurred at a high-order sublevel of the quantum dots. This may be because the optical gain was small due to the low areal coverage and single dot layer. The numerical density of the ALS dots was about 5%, and multiple stacking of dot layers has not yet been achieved. Increasing the areal coverage and the number of dot layers would lead to lasing at a lower sublevel, resulting in excellent performance. A high areal coverage and multiple dot layers have been achieved in the columnar dots.

3.2 Columnar-dot lasers

Double heterostructure lasers with two (N = 2) columnar-dot layers were fabricated. The schematic of the laser structure is shown in **Figure 9**. The laser structures were grown on a (001) n-GaAs substrate followed by a 1.4 µm n-$Al_{0.4}Ga_{0.6}As$ cladding layer, a quantum-dot active layer, a 1.4 µm p-$Al_{0.4}Ga_{0.6}As$ cladding layer, and a 0.4 µm p-GaAs contact layer. The columnar-dot layers were separated by a 30 nm GaAs layer and sandwiched by GaAs separate confinement heterostructure (SCH) layers. We formed 3 µm-wide and 1.2 µm-high ridge structures by chemical etching. The cavity lengths (L) were 300 µm and 900 µm.

Room temperature continuous wavelength (CW) operation was achieved with a laser having L = 900 µm. **Figure 10** shows the light output

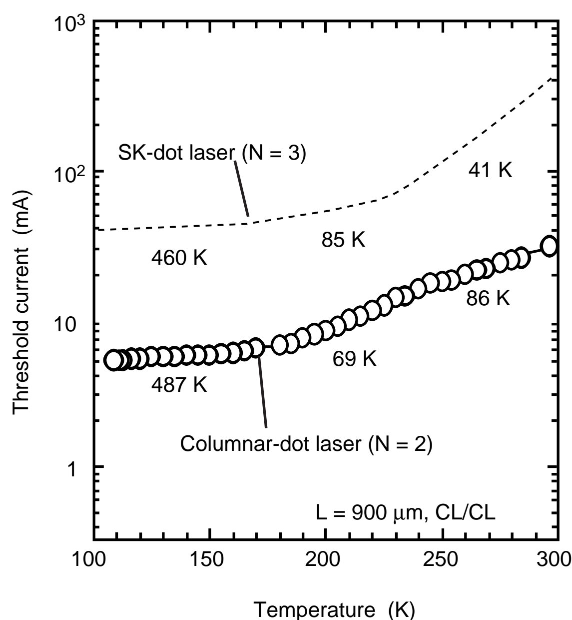

Figure 11
Threshold current of columnar-dot laser as a function of temperature.

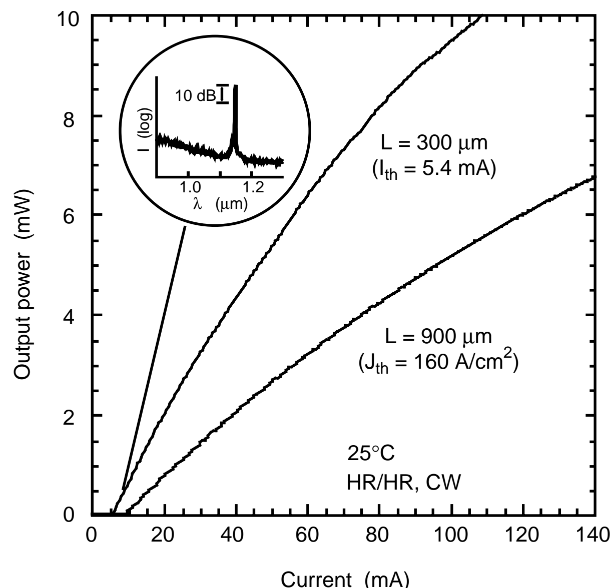

Figure 12
L-I characteristics of columnar-dot lasers with *L* = 300 and 900 μm and HR coating on both facets.

versus current characteristic. The threshold current was 31 mA,[42] which is more than one order of magnitude smaller than that of our SK-dot lasers with the common laser structure (520 mA).[27] The lasing spectrum is shown in the inset of Figure 10. Comparing the lasing wavelength with the PL wavelength (Figure 5), we assigned the lasing level to the second level. A high output power of 42 mW was obtained at an injected current of 150 mA. The external quantum efficiency, η_d, was 36%, which did not decrease much as the temperature was increased (η_d = 30% at 70°C). From the value at 25°C, we roughly estimated the internal loss of the laser structure. The differential internal efficiency (η_i) has been reported as being 70% for an $In_{0.5}Ga_{0.5}As$ quantum-dot laser and 81% for an $In_{0.3}Ga_{0.7}As$ quantum-dot laser.[26] Assuming that the reflectivity of the cleaved facet was 30% for the columnar-dot laser, the internal loss is calculated to be about 3.5 cm^{-1} with η_i = 90%, and about 5.5 cm^{-1} with η_i = 100%. Therefore, we can expect to achieve an ultra-low internal loss and a high differential internal efficiency in the columnar-dot laser.

Figure 11 shows the temperature dependence of the threshold current. An excellent characteristic temperature (T_0) of about 500 K was obtained at low temperature. The T_0 of 69 K was obtained between 180 K and 240 K, at which point the threshold current increased following the lasing level shift from the ground level to the second level. At near room temperature, the T_0 was over 80 K, which is about twice that of our SK-dot lasers.[27] However, the value near room temperature is significantly smaller than the expected value for quantum-dot lasers. We assume that there are two factors dominating the temperature characteristics. The first one is related to the PL intensity. The PL intensity is dependent on temperature, especially in the high-temperature region, reflecting the decrease in the emission efficiency. This decrease in emission efficiency requires the additional injection of carriers into the quantum dots, which results in a proportional increase in the threshold current. The second factor is the thermal excitation of carriers to the second sublevel. The energy separation between the ground level and the second level is 45 meV.

As shown in Figure 5, the carrier distribution to the second level cannot be neglected at room temperature. To further improve the temperature characteristics, we must optimize the energy separation between the sublevels of quantum dots as well as improve the emission efficiency.

An even lower threshold current and higher output power were achieved from columnar-dot lasers with HR-coated facets[43]. For a laser with a cavity length of 300 µm and HR coating on both facets, lasing oscillation occurred at a threshold current of 5.4 mA at 25°C (**Figure 12**). For a laser with L = 900 µm and HR coating on both facets, we calculated that the threshold current density was as low as 160 A/cm^2 by assuming, based on the near field pattern, that the current injection area was about twice the ridge width. The lasing occurred at the ground level in these devices. For a laser with L = 900 µm and HR coating on one side of the facets, an output power of 110 mW was achieved (**Figure 13**). Even at 70°C, an output power of 75 mW was obtained. To our knowledge, such a low threshold current and high output power have never been reported for edge-emitting quantum-dot lasers.

Figure 14 shows the EL and lasing spectra of lasers with as-cleaved facets and a cavity length of 300 µm. Clear differences can be observed in the spectra between 110 K and 298 K. At 298 K, the threshold current is large, and the EL spectra below threshold have an asymmetric shape. Near room temperature, the threshold carrier density is large because of nonradiative recombination and thermal excitation of carriers. The EL peak shifts to the shorter wavelength side as the injection current is increased. The lower threshold currents at lower temperatures lead to reduced broadening of the EL spectra, resulting in suppressed emission from higher-order sublevels. The EL

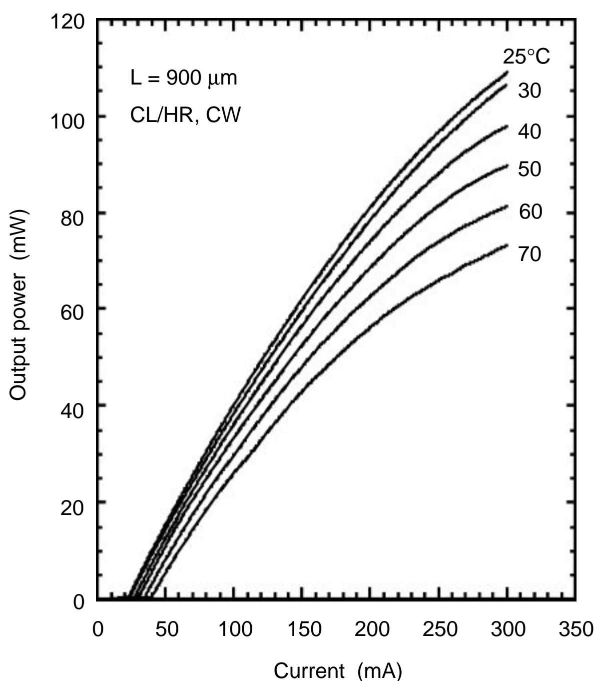

Figure 13
L-I characteristics of columnar-dot laser with L = 900 µm and HR coating on one facet at temperatures between 25 and 70°C.

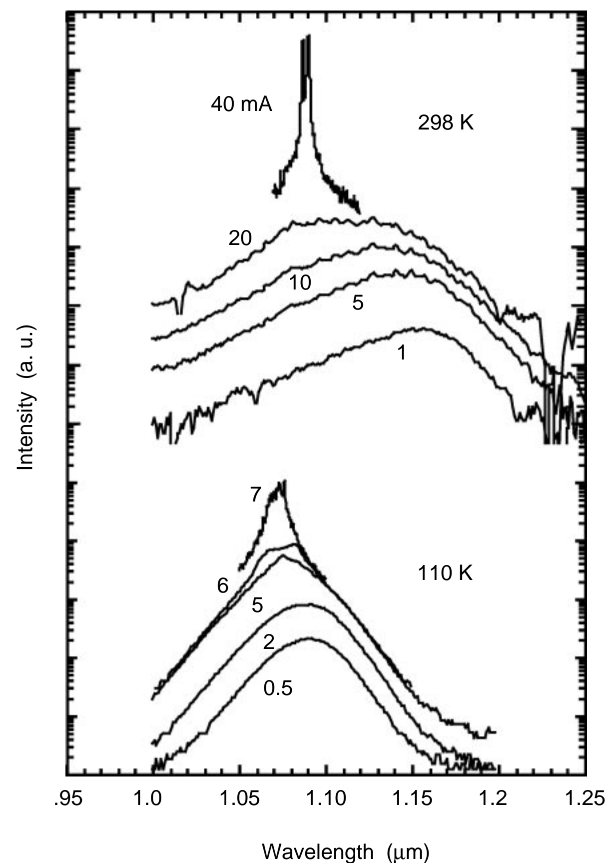

Figure 14
Lasing spectra and EL spectra of columnar-dot laser at 110 K and 298 K.

spectrum at 110 K is nearly symmetric and is attributed to the reduction of threshold carrier density and the suppression of thermal excitation of carriers into higher-order sublevels. The threshold current density is about 80 A/cm^2, which is about one order of magnitude smaller than that of the ALS-dot laser.

Lasing occurred at many wavelengths at 110 K. This was not the multi-mode oscillation observed in ordinary Fabry-Perot lasers. Various quantum dots with different sizes and compositions were simultaneously lasing, since the gains in the various dots can reach the threshold due to decreased nonradiative carrier recombination at 110 K. The wavelength span became smaller as the temperature was increased. This result gives a clear indication that each quantum dot is spatially separated but optically coupled. Also, it suggests the possibility that operation may be possible at even lower threshold currents if the uniformity of the quantum dots is greatly improved to enable lasing in narrower wavelength ranges.

We suspect that the high uniform energy levels and rare nonradiative emission in the columnar dots were the decisive factors that enabled us to achieve a high gain from a quantum-dot laser structure. In addition, we think that the electrically-coupled wetting layers increased the rate of carrier injection into the dots by acting as a carrier reservoir. (We have discussed whether the closely stacked wetting layers around the dots are electrically coupled.) Carriers were possibly more easily captured by the deep and wide wetting layers than by the single (and therefore, shallow) wetting layer of SK dots. The deeper the wetting layers, the more strongly restricted is the thermal carrier diffusion from the wetting layers to GaAs layers. The good carrier capture efficiency contributes to the high output power. Moreover, the high areal coverage and multiple dot layers provide advantages over the ALS dots.

5. Conclusion

This paper reported on the low threshold current and high output power of self-assembled quantum-dot lasers. The uniformity and emission efficiency of dots fabricated by MOVPE (ALS dots) and MBE (columnar dots) were improved by growing the dots with alternate supply of InAs and GaAs on a GaAs substrate. We showed that the improved uniformity, emission efficiency, and numerical density of these quantum dots greatly improve the performance of quantum-dot lasers. Using the columnar dots, we achieved the following records for edge-emitting quantum-dot lasers: a low threshold current of 5.4 mA, and a high output power of 110 mW. The static performance of quantum-dot lasers is comparable with that of quantum-well lasers. One of the most important issues regarding dot lasers for the near future is 1.3 µm lasing. Since 1.3 µm emission of the ground level has been achieved by ALS dots, we believe that the alternate supply technique is promising.

Acknowledgements

The authors would like to thank Dr. Hajime Shoji, Dr. Hiroshi Ishikawa, and Dr. Naoki Yokoyama for their helpful advice and Mr. Koji Otsubo for his technical assistance. We also would like to thank Mr. Toshiro Futatsugi and Mr. Yoshihiro Sugiyama for the fruitful discussion we had with them.

References

1) L. Brus: Zero-Dimensional Excitons in Semiconductor Clusters. *IEEE J. Quantum Electron*, **QE-22**, pp.1909-1914 (1986).
2) D. S. Chemla and D. A. B. Miller: Mechanism for enhanced optical nonlinearities and bistability by combined dielectric-electronic confinement in semiconductor microcrystallites. *Opt. Lett.*, **11**, pp.522-524 (1986).
3) Y. Arakawa and H. Sakaki: Multidimensional quantum well laser and temperature dependence of its threshold current. *Appl. Phys. Lett.*, **40**, 11, pp.939-941 (1982).

4) M. Asada, Y. Miyamoto, and Y. Suematsu: Gain and the Threshold of Three-Dimensional Quantum-Box Lasers. *IEEE J. Quantum Electron.*, **QE-22**, pp.1915-1921 (1986).
5) H. Sakaki: Quantum Wire Superlattices and Coupled Quantum Box Arrays: A Novel Method to Suppress Optical Phonon Scattering in Semiconductors. *Jpn. J. Appl. Phys*. **28**, pp.L314-L316 (1989).
6) K. J. Vahala: Quantum box fabrication tolerance and size limits in semiconductors and their effect on optical gain. *IEEE J. Quantum Electron.*, **24**, pp.523-530 (1988).
7) M. Grundmann, J. Christen, N. N. Ledentsov, J. Böhrer, D. Bimberg, S. S. Ruvimov, P. Werner, U. Richter, U. Gösele, J. Heydenreich, V. M. Ustinov, A. Yu. Egorov, A. E. Zhukov, P. S. Kop'ev, and Zh. I. Alferov: Ultranarrow luminescence lines from single quantum dots. *Phys. Rev. Lett.*, **74**, pp.4043-4046 (1995).
8) K. Kash, A. Scherer, J. M. Worlock, H. G. Craighead, and M. C. Tamargo: Optical spectroscopy of ultrasmall structures etched from quantum wells. *Appl. Phys. Lett*. **49**, pp.1043-1045 (1986).
9) T. Fukui, S. Ando, Y. Tokura, and T. Toriyama: GaAs tetrahedral quantum dot structures fabricated using selective area metalorganic chemical vapor deposition. *Appl. Phys. Lett.*, **58**, pp.2018-2020 (1991).
10) H. Hirayama, K. Matsunaga, M. Asada, and Y. Suematsu: Lasing action of GaInAs/GaInAsP/InP tensile-strained quantum-box lasers. *Electron. Lett.*, **30**, pp.142-143 (1994).
11) M. Tabuchi, S. Noda, and A. Sasaki: Science and Technology of Mesoscopic Structures. edited by S. Namba, C. Hamaguchi, and T. Ando, Springer Tokyo, p.379, 1992.
12) H. Takagi, H. Ogawa, Y. Yamazaki, A. Ishizaki, and T. Nakagiri: Quantum size effects on photoluminescence in ultrafine Si particles. *Appl. Phys. Lett.*, **56**, pp.2379-2380 (1990).
13) R. Apetz, L. Vescan, A. Hartmann, C. Dieker, and H. Lüth: Photoluminescence and electroluminescence of SiGe dots fabricated by island growth. *Appl. Phys. Lett.*, **66**, pp.445-447 (1995).
14) J. M. Moison, F. Houzay, F. Barthe, L. Lepeince, E. Andre, and O. Vatel: Self-organized growth of regular nanometer-scale InAs dots on GaAs. *Appl. Phys. Lett.*, **64**, pp.196-198 (1994).
15) D. Leonard, M. Kishnamurthy, C. M. Reaves, S. P. Denbaars, and P. M. Petroff: Direct formation of quantum-sized dots from uniform coherent islands of InGaAs on GaAs surfaces. *Appl. Phys. Lett.*, **63**, 23, pp.3203-3205 (1993).
16) R. Nötzel, J. Temmyo, H. Kamada, T. Furuta, and T. Tamamura: Strong photoluminescence emission at room temperature of strained InGaAs quantum disks (200-300 nm diameter) self-organized on GaAs (311)B substrates. *Appl. Phys. Lett.*, **65**, 4, pp.457-459 (1994).
17) J. Oshinowo, M. Nishioka, S. Ishida, and Y. Arakawa: Highly uniform InGaAs/GaAs quantum dots (~15 nm) by metalorganic chemical vapor deposition. *Appl. Phys. Lett.*, **65**, 11, pp.1421-1423 (1994).
18) K. Mukai, N. Ohtsuka, M. Sugawara, and S. Yamazaki: Self-formed $In_{0.5}Ga_{0.5}As$ quantum dots on GaAs substrates emitting at 1.3 µm. *Jpn. J. Appl. Phys.*, **33**, 12A, pp.L1710-L1712 (1994).
19) A. Moritz, R. Wirth, A. Hangleiter, A. Kurtenbach, and K. Eberl: Optical gain and lasing in self-organized InP/GaInP quantum dots. *Appl. Phys. Lett.*, **69**, pp.212-214 (1996).
20) F. Hatami, N. N. Ledentsov, M. Grundmann, J. Böhrer, F. Heinrichsdorff, M. Beer, D. Bimberg, S. S. Ruvimov, P. Werner, U. Gösele, J. Heydenreich, S. V. Ivanov, B. Ya. Meltser, P. S. Kop'ev, and Zh. I. Alferov: Radiative recombination in type-II GaSb/GaAs quantum dots. *Appl. Phys. Lett.*, **67**, pp.656-658 (1995).
21) E. R. Glaser, B. R. Benett, B. V. Shanabrook, and R. Magno: Photoluinescence studies of self-assembled InSb, GaSb, and AlSb quan-

tum dot heterostructures. *Appl. Phys. Lett.*, **68**, pp.3614-3616 (1996).

22) H. C. Ko, D. C. Park, Y. Kawakami, S. Fujita, and S. Fujita: Self-organized CdSe quantum dots onto cleaved GaAs (110) originating from Stranski-Krastanow growth mode. *Appl. Phys. Lett.* **70**, pp.3278-3280 (1997).

23) S. Tanaka, S. Iwai, and Y. Aoyagi: Self-assembling GaN quantum dots on Al_x Ga_{1-x} N surfaces using a surfactant. *Appl. Phys. Lett.*, **69**, pp.4096-4098 (1996).

24) N. Kirstaedter, N. N. Ledentsov, M. Grundmann, D. Bimberg, V. M. Ustinov, S. S. Ruvimov, M. V. Maximov, P. S. Kop'ev, Zh. I. Alferov, U. Richter, P. Werner, U. Göele, and J. Heydenreich: Low threshold, large T_0 injection laser emission from (InGa)As quantum dots. *Electron. Lett.*, **30**, 17, pp.1416-1417 (1994).

25) H. Shoji, K. Mukai, N. Ohtsuka, M. Sugawara,T. Uchida, and H. Ishikawa: Lasing at three-dimensionally quantum confined sublevel of self-organized $In_{0.5}Ga_{0.5}As$ quantum dots by current injection. *IEEE Photon. Technol. Lett.*, **12**, pp.1385-1387 (1995).

26) D. Bimberg, N. Kirsteadter, N. N. Ledentsov, Zh. I. Alferof, P. S. Kop'ev, and V. M. Ustinov : InGaAs-GaAs Quantum-Dot Lasers. *IEEE J. of selected topics in quantum electron.*, **3**, pp.196-205 (1997).

27) H. Shoji, Y. Nakata, K. Mukai, Y. Sugiyama, M. Sugawara, N. Yokoyama, and H. Ishikawa: Room Temperature CW Operation at The Ground State of Self-Formed Quantum Dot Lasers with Multi-Stacked Dot Layer. *Electron. Lett.*, **32**, pp.2023-2024 (1996).

28) F. Heinrichsdorff, M.-H. Mao., N. Kirstaedter, A. Krost, and D. Bimberg: Room-temperature continuous-wave lasing from stacked InAs/GaAs quantum dots by metalorganic chemical vapor deposition. *Appl. Phys. Lett.*, **71**, pp.22-24 (1997).

29) M. Ozeki, N. Ohtsuka, and Y. Sakuma: Pulsed-Jet Epitaxy of III-V Compounds. *FUJITSU Sci. Tech. J.*, **28**, pp.50-61 (1992).

30) N. Ohtsuka, and O. Ueda: Growth of InAs and $(InAs)_1(GaAs)_1$ superlattice quantum well structures on GaAs by atomic layer epitaxy using trimethylindium-dimethylethylamine adduct. *Mat. Res. Soc. Symp. Proc.*, **334**, pp.225-229 (1994).

31) K. Mukai, N. Ohtsuka, and M. Sugawara: Controlled Quantum Confinement Potentials in Self-Formed InGaAs Quantum Dots Grown by Atomic Layer Epitaxy Technique. *Jpn. J. Appl. Phys.*, **35**, pp.L262-L265 (1996).

32) N. Grandjean and J. Massies: Epitaxial growth of highly strained $In_xGa_{1-x}As$ on GaAs(001): the role of surface diffusion length. *J. Cryst. Growth*, **134**, pp.51-62 (1993).

33) J. Osaka, N. Inoue, Y. Mada, K. Yamada and K. Wada: In-situ observation of roughening process of MBE GaAs surface by scanning reflection electron microscopy. *J. Cryst. Growth*, **99**, pp.120-123 (1990).

34) P. Boguslawski and A. Baldereschi: Excess elastic energy and the instability of bulk and epitaxial lattice-mismatched monolayer (001) superlattices. *Phys. Rev. B*, **39**, pp.8055-8058 (1989).

35) Y. Sakuma, M. Ozeki, and K. Nakajima: Arsenic desorption from the InAs(001) growth surface during atomic layer epitaxy. *J. of Cryst. Growth*, **130**, pp.147-152 (1993).

36) K-N. Tu, J. W. Mayer, and L. C. Feldman: Electronic Thin Film Science for Electrical Engineers and Material Scientists. Macmillan Publishing Company, New York, 1992.

37) Y. Nakata, Y. Sugiyama, T. Futatsugi, and N. Yokoyama: Self-assembled structures of closely stacked InAs islands grown on GaAs by molecular beam epitaxy. *J. Crystal Growth*, **175/176**, pp.713- 719 (1997).

38) Y. Sugiyama, Y. Nakata, K. Imamura, S. Muto, and N. Yokoyama: Stacked InAs self-assembled quantum dots on (001) GaAs grown by molecular beam epitaxy. *Jpn. J. Appl. Phys.*, **35**, pp.1320-1324 (1996).

39) M. Sugawara, Y. Nakata, K. Mukai, and H. Shoji: Exciton diamagnetic shifts in self-formed closely stacked InAs/GaAs quantum dots. *Phys. Rev. B*, **55**, pp.13155-13160 (1997).
40) H. Shoji, Y. Nakata, K. Mukai, Y. Sugiyama, M. Sugawara, N. Yokoyama, and H. Ishikawa: Application of Narrow Emission Spectrum Closely-Stacked Structure to Quantum Dot Lasers. technical digest of 2nd Opt. and Commun. Conf., 1997, Seoul, Korea, pp.176-177.
41) Y. Nakata, Y. Sugiyama, T. Futatsugi, K. Mukai, H. Shoji, M. Sugawara, H. Ishikawa, and N. Yokoyama: MBE-growth of closely stacked InAs islands. (in Japanese), Ext. Abs. The 58th Autumn Meeting of The Japan Society of Applied Physics, 2pM-4, p.233, 1997.
42) K. Mukai, Y. Nakata, H. Shoji, M. Sugawara, K. Ohtsubo, N. Yokoyama, and H. Ishikawa: Low threshold CW lasing of closely-stacked self-organiged InAs/GaAs quantum dots. Proceeding of 10th Indium Phosphide and Related Materials (IPRM'98), pp.345-348, 1998.
43) K. Mukai, Y. Nakata, H. Shoji, M. Sugawara, K. Ohtsubo, N. Yokoyama, and H. Ishikawa: Lasing with low threshold current and high output power from colummar-shaped InAs/GaAs quantum dots. *Electron. Lett.*, **34**, pp. 1588-1590 (1998).

Kohki Mukai received a B.S. degree from Kyoto University, Japan in 1986. He joined the Research and Development Laboratories of Kanebo Ltd., Osaka, Japan in 1986. In 1990, he joined Fujitsu Laboratories Ltd., where he has been engaged in the research and development of compound semiconductor materials for optoelectronic device applications. Mr. Mukai is a member of the Japan Society of Applied Physics and the Physical Society of Japan.

E-mail : kmukai@flab.fujitsu.co.jp

Yoshiaki Nakata was born in Nagano, Japan in 1960. He recevied B.E. and M.E. degrees from Tokyo University of Agriculture and Technology, Tokyo, Japan in 1983 and 1985, respectively. He joined Fujitsu Laboratories Ltd. in 1985. Since then, he has been engaged in research on molecular beam epitaxy of III-V compound semiconductors. Mr. Nakata is a member of the Japan Society of Applied Physics.

E-mail : nakata@qed.flab.fujitsu.co.jp

Mitsuru Sugawara received B.E. and M.E. degrees from the University of Tokyo in1982 and 1984, respectively. He joined Fujitsu Laboratories Ltd. in 1984. He received the Ph.D. degree in Engineering from the University of Tokyo in 1994. He has been engaged in experimental and theoretical research on the optical properties of low dimensional quantum nano-structures and their device applications. Dr. Sugawara is a member of the Japan Society of Applied Physics and the American Physical Society.

E-mail : msuga@flab.fujitsu.co.jp